

# Optical Clearing of Plant Tissues for Fluorescence Imaging

Daisuke Kurihara<sup>1</sup>, Yoko Mizuta<sup>1,2</sup>, Shiori Nagahara<sup>1</sup>, Yoshikatsu Sato<sup>1,3</sup>, Tetsuya Higashiyama<sup>1,3,4</sup>

<sup>1</sup> Institute of Transformative Bio-Molecules (ITbM), Nagoya University <sup>2</sup> Institute for Advanced Research (IAR), Nagoya University <sup>3</sup> Division of Biological Science, Graduate School of Science, Nagoya University <sup>4</sup> Department of Biological Sciences, Graduate School of Science, The University of Tokyo

## Corresponding Author

Daisuke Kurihara

kuri@bio.nagoya-u.ac.jp

## Citation

Kurihara, D., Mizuta, Y., Nagahara, S., Sato, Y., Higashiyama, T. Optical Clearing of Plant Tissues for Fluorescence Imaging. *J. Vis. Exp.* (179), e63428, doi:10.3791/63428 (2022).

## Date Published

January 5, 2022

## DOI

10.3791/63428

## URL

jove.com/video/63428

## Abstract

It is challenging to directly observe the internal structure of multi-layered and opaque plant specimens, without dissection, under a microscope. In addition, autofluorescence attributed to chlorophyll hampers the observation of fluorescent proteins in plants. For a long time, various clearing reagents have been used to make plants transparent. However, conventional clearing reagents diminish fluorescent signals; therefore, it has not been possible to observe the cellular and intracellular structures with fluorescent proteins. Reagents were developed that can clear plant tissues by removing chlorophyll while maintaining fluorescent protein stability. A detailed protocol is provided here for the optical clearing of plant tissues using clearing reagents, ClearSee (CS) or ClearSeeAlpha (CSA). The preparation of cleared plant tissues involves three steps: fixation, washing, and clearing. Fixation is a crucial step in maintaining the cellular structures and intracellular stability of fluorescent proteins. The incubation time for clearing depends on the tissue type and species. In *Arabidopsis thaliana*, the time required for clearing with CS was 4 days for leaves and roots, 7 days for seedlings, and 1 month for pistils. CS also required a relatively short time of 4 days to make the gametophytic leaves of *Physcomitrium patens* transparent. In contrast, pistils in tobacco and *torenia* produced brown pigment due to oxidation during CS treatment. CSA reduced the brown pigment by preventing oxidation and could make tobacco and *torenia* pistils transparent, although it took a relatively long time (1 or 2 months). CS and CSA were also compatible with staining using chemical dyes, such as DAPI (4',6-diamidino-2-phenylindole) and Hoechst 33342 for DNA and Calcofluor White, SR2200, and Direct Red 23 for the cell wall. This method can be useful for whole-plant imaging to reveal intact morphology, developmental processes, plant-microbe interactions, and nematode infections.

## Introduction

Visualization of cellular structures and localization of proteins in living organisms is important for clarifying their functions *in vivo*. However, since the living body is not transparent, it is challenging to observe the internal structure of living organisms without dissection. Especially, in the case of plant tissues, which are multi-layered with cells of different shapes, the index mismatch caused by their structure and the presence of light-absorbing pigments is problematic. For example, plant leaves have a complex structure that allows them to efficiently utilize the light that enters their bodies for photosynthesis<sup>1</sup>, whereas the structure also causes refractive index mismatch, making them difficult to observe. However, leaves have many light-absorbing pigments, such as chlorophyll, which emit strong red fluorescence and brownish pigments are produced by oxidation<sup>2,3</sup>. These pigments also hinder whole-mount fluorescence microscopy observations in plants. Therefore, for observing the internal structure of plants, decolorization and fixation by alcohol and clearing using chloral hydrate have been used for a long time to eliminate the refractive index mismatch and autofluorescence<sup>4,5</sup>. These conventional methods have been adopted for many years, but they have the drawback of eliminating the fluorescence of fluorescent proteins at the same time<sup>6,7</sup>. This is problematic since fluorescent proteins have become indispensable in current fluorescent imaging.

Therefore, ClearSee (CS) and ClearSeeAlpha (CSA) have been developed as optical clearing reagents for plant tissues. Both reagents reduce chlorophyll autofluorescence while maintaining the stability of fluorescent proteins<sup>7,8</sup>. CSA is particularly useful when brown pigments are produced owing to tissue oxidation. Using these clearing reagents,

it is possible to observe the cellular structure and protein localization inside the plant body without physical sectioning.

## Protocol

### 1. Preparation of clearing solutions

1. To prepare CS solution, dissolve 10% (w/v) xylitol, 15% (w/v) sodium deoxycholate, and 25% (w/v) urea in distilled water on a magnetic stirrer.

**NOTE:** Sodium deoxycholate powder should be weighed in a draft chamber as it easily floats in the air. CS can be stored at room temperature in dark for more than 1 year.

2. To prepare CSA solution, add sodium sulfite (50 mM final concentration) to the CS solution obtained above.

**NOTE:** Add sodium sulfite to the CS solution right before use as the reducing agent gets deactivated easily.

### 2. Preparation of the fixative solution

1. Transfer 40 mL of sterilized water into a conical tube and add 2 g of paraformaldehyde. Add 200  $\mu$ L of 2 N NaOH to increase the pH of the solution. After closing and sealing the tube with parafilm, incubate at 60 °C with occasional inversions until everything is dissolved.
2. After cooling the solution to room temperature, add 5 mL of 10x phosphate-buffered saline (PBS) to adjust the pH to 7.4. Add sterilized water to make up the volume to 50 mL.

**NOTE:** A freshly prepared fixative solution is preferred. The solution can also be stored at -30 °C for several months.

### 3. Fixation of samples

1. Immerse plant samples in the fixative solution in a microtube (**Figure 1A**), ensuring that the volume of the fixative solution is more than five times the sample volume.
2. Seal the microtube with a parafilm and make holes using a needle. Do not leave the tube open owing to a risk of sample spillage during vacuum decompression.
3. Place the microtube in a desiccator and slowly adjust the degree of vacuum (~690 mmHg) so that bubbles appear gradually from the samples (**Figure 1B-C**). Turn off the vacuum pump after evacuating the desiccator. Leave the microtube undisturbed for 30 min at room temperature.
4. Vent the desiccator carefully to prevent disturbing the samples. Turn on the vacuum pump again and turn it off after evacuating the desiccator. Leave the microtube undisturbed for 30 min at room temperature.

**NOTE:** Care should be taken to prevent damage to the samples while venting the desiccator. The penetration of the fixative solution into the samples is enhanced by two vacuum treatments. Further vacuum treatment helps to penetrate the fixative solution into thicker samples.

5. Open the desiccator carefully without bumping the fixative solution in the microtube. Using a micropipette, remove the fixative solution and add 1x PBS. After storing for 1 min, replace the old PBS with new 1x PBS (**Figure 1D**).

### 4. Clearing

1. After removing PBS, add five times the sample volume of the clearing solution.
2. Seal the microtube with parafilm and make holes using a needle. Place the samples in the desiccator, evacuate as in step 3.3, and turn off the vacuum pump. Leave the microtube undisturbed for 60 min at room temperature.
3. Open the desiccator gently. Close the microtube with parafilm and store it at room temperature in the dark to avoid photobleaching of fluorescent proteins. Invert the microtube every 1-2 days to accelerate the clearing process.
4. When the clearing solution turns green, replace it with new clearing solutions until the solution remains colorless (**Figure 1E-H**).

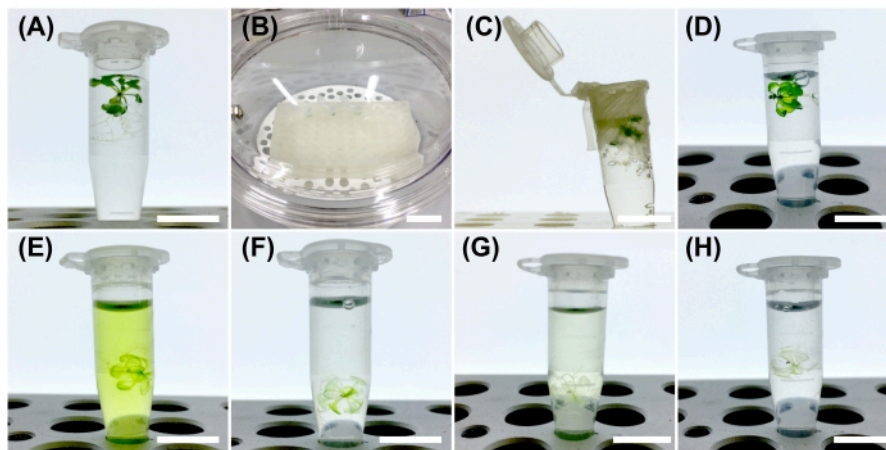


**Figure 1: Procedure for CS treatment.** (A) *Arabidopsis* seedling in 4% PFA (Paraformaldehyde) solution. (B) The sample is placed into a desiccator. (C) The seedling is fixed under a vacuum. (D) The seedling is soaked in the PFA solution after vacuum treatment. (E) Resulting 3-day clearing solution-treated seedling. Note the green color of the clearing solution. (F) The clearing solution is replaced 3 days after treatment. (G) Resulting 5-day clearing solution-treated seedling. (H) The clearing solution is replaced 5 days after treatment. Scale bars: 1 cm (A,C-H) and 5 cm (B). [Please click here to view a larger version of this figure.](#)

## 5. Chemical dye staining

- To the microtube, add Hoechst 33342 (final concentration of 10  $\mu\text{g}/\text{mL}$ ) for nuclear staining or Calcofluor White (final concentration of 1  $\text{mg}/\text{mL}$ ) for cell wall staining and wait for 1 h. After removing the dye solution, wash the sample with a fresh clearing solution for 1 h.

**NOTE:** Overnight staining and washing can improve fluorescent dye penetration into tissues and reduce background fluorescence. Various fluorescent dyes are compatible with the CS solution such as Basic Fuchsin<sup>9</sup> (lignin), Auramine O<sup>9</sup> (lignin, suberin, and cutin), Nile Red<sup>9</sup> (suberin), Direct Yellow 96<sup>9</sup>, Direct Red 23<sup>9</sup>, and SR2200<sup>10,11</sup> (cell walls).

## 6. Observation

- Cut silicone rubber sheet with a razor blade to prepare a frame for the spacer (**Figure 2A**).  
**NOTE:** Adjust the thickness of the silicon rubber sheet according to the thickness of the sample. As samples treated with clearing solution are soft, they will be damaged if they are covered directly with the cover glass.
- Place the silicone frame on cover glass (e.g., 25 x 60 mm) (**Figure 2B**). Place the treated samples within the frame and add ~100  $\mu\text{L}$  of clearing solution to remove any bubbles in the frame. Cover with another cover glass (18 x 18 mm or 24 x 24 mm) to prevent evaporation of the clearing solution (**Figure 2C**).

- Observe the samples under a fluorescent microscope.  
After observation, return the samples to the clearing

solution taken in a microtube and store at room temperature in the dark.

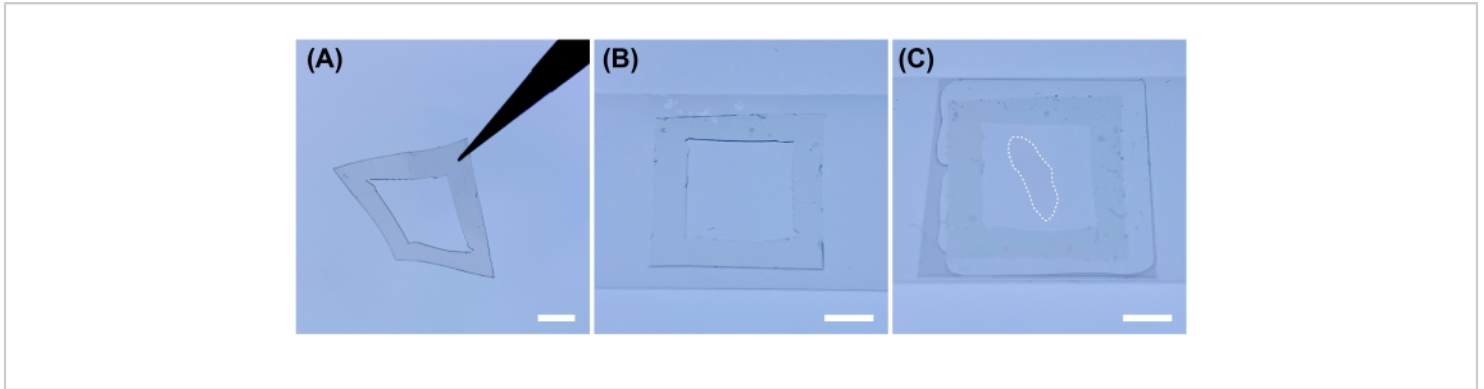


**Figure 2: Sample preparation for microscopic observation.** (A) Cut a 0.2 mm thick silicone sheet into a frame. (B) Put the silicone sheet frame onto the cover glass. (C) Place the sample treated with clearing solution (marked by dotted border) within the frame and cover it with a cover glass. Scale bars: 5 mm. [Please click here to view a larger version of this figure.](#)

## Representative Results

CS can clear leaves of various species (**Figure 3A-H**). It is difficult for the CS solution to penetrate a rice leaf because the leaf surface is covered by cuticular wax in this plant. However, after extracting the cuticular wax by dipping in chloroform for 10 s, CS could clear the rice leaves (**Figure 3H**). CS could not, however, penetrate *Chamaecyparis obtusa* leaves which are less permeable to CS (**Figure 3I,J**). In *Chrysanthemum* leaves, brown pigmentation induced by polyphenol oxidation was observed in the CS-treated leaves (**Figure 3K,L**). Similarly, Tobacco and torenia pistils showed brown pigmentation during the CS treatment (**Figure 3M,O**). As the sodium sulfite component in CSA prevents polyphenol oxidation owing to the reducing effect, CSA could clear tobacco and torenia pistils without any brown pigmentation (**Figure 3N,P**).

**Figures 4B** shows that CS treatment reduced the pale green color of the *Arabidopsis* H2B-mClover leaf (bright field)

and enhanced the fluorescence intensity of H2B-mClover compared with PBS incubation (**Figure 4A**). In addition to flowering plants, CS is also applicable to moss plants (**Figure 4C**); after 4 days of CS treatment, the fluorescence of H2B-mRFP was clearly detected for the entire gametophore with reduced chlorophyll autofluorescence. **Figures 4D,E** show 3D reconstruction images of the H2B-mClover pistil in *Nicotiana benthamiana* cleared using CSA. The sample depth was 440  $\mu\text{m}$ . As the depth-coded maximum intensity projection image shows, CSA allows for deep imaging of challenging tissues, such as tobacco pistils.

CS and CSA were also compatible with fluorescent dye staining. **Figure 5** shows that CS could simultaneously be used to observe the fluorescent protein (H2B-mClover) and organic fluorescent dye staining (Calcofluor White). After 3D reconstruction from the z-stack images, any section could be observed.

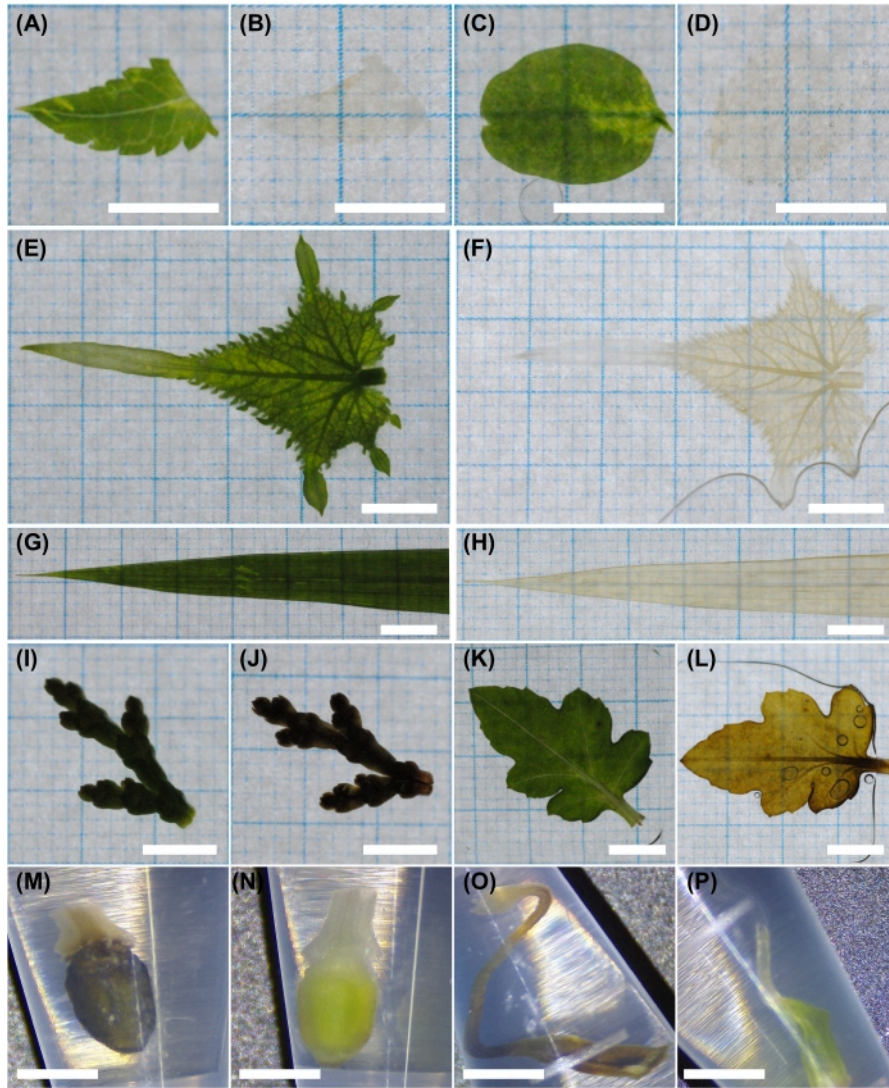


**Figure 3: Optical clearing of leaves and pistils using clearing solutions.** (A-L) Fixed leaves of various species were incubated in PBS (A,C,E,G,I,K) or CS (B,D,F,H,J,L) for 8 days and CS (M,O) or CSA (N,P) for 2 days. (A,B,O,P) *Torenia fournieri*, (C,D) *Nicotiana tabacum*, (E,F) *Cucumis sativus*, (G,H) *Oryza sativa*, (I,J) *Chamaecyparis obtusa*, (K,L) *Chrysanthemum morifolium*, (M,N) *Nicotiana benthamiana*. Scale bars: 1 cm. [Please click here to view a larger version of this figure.](#)

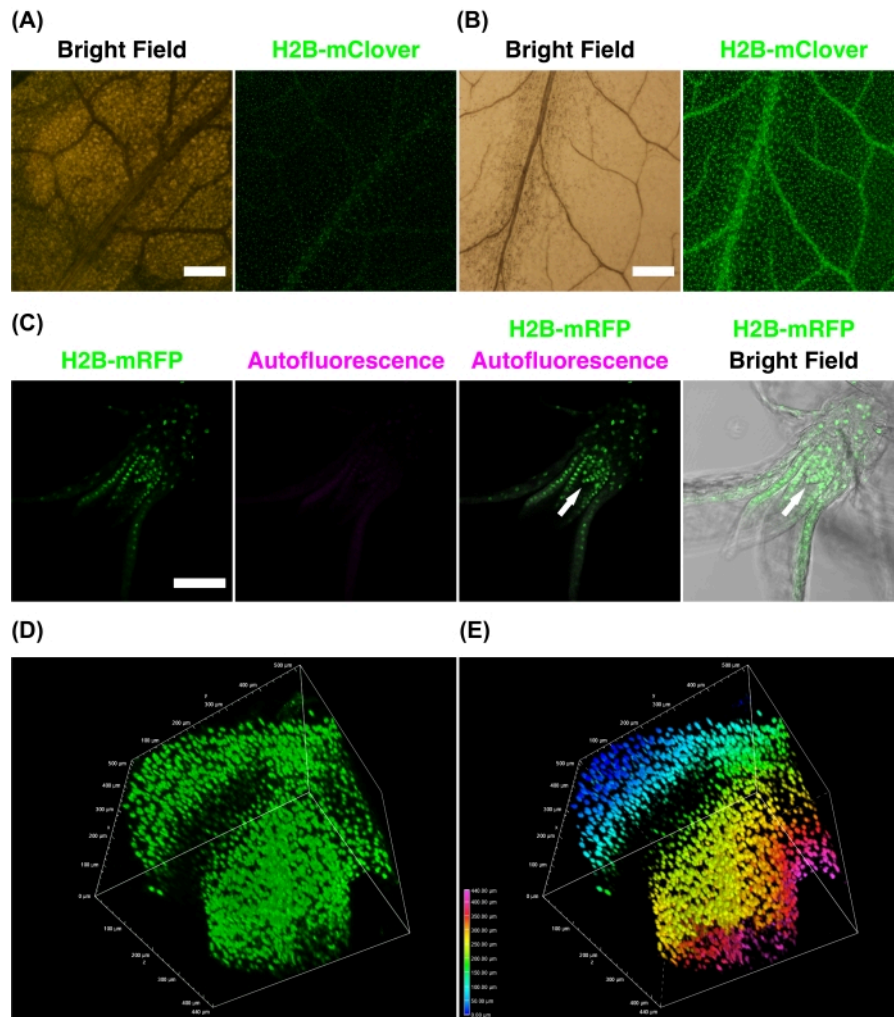


**Figure 4: Fluorescence imaging of tissues treated with clearing solutions.** (A,B) UBQ10pro::H2B-mClover leaves of *Arabidopsis thaliana* were treated with PBS (A) or CS (B) for 3 days. (C) H2B-mRFP leafy gametophores of *Physcomitrium patens* were treated with CS for 4 days. The nuclei were labeled with H2B-mRFP (green). The CS treatment reduced chlorophyll autofluorescence (magenta). The H2B-mRFP signal in the apical region was clearly observed for both merged images of H2B-mRFP and autofluorescence or bright field. (D,E) The UBQ10pro::H2B-mClover stigma of *Nicotiana benthamiana* was treated in CSA for 1 month. Maximum-intensity projection (D) and depth-coded maximum-intensity projection (E) were generated from 88 z-stack images at 5 μm intervals. Scale bars: 100 μm. Images were taken using wide-field (A,B), confocal (C), and two-photon excitation (D,E) microscopy. [Please click here to view a larger version of this figure.](#)

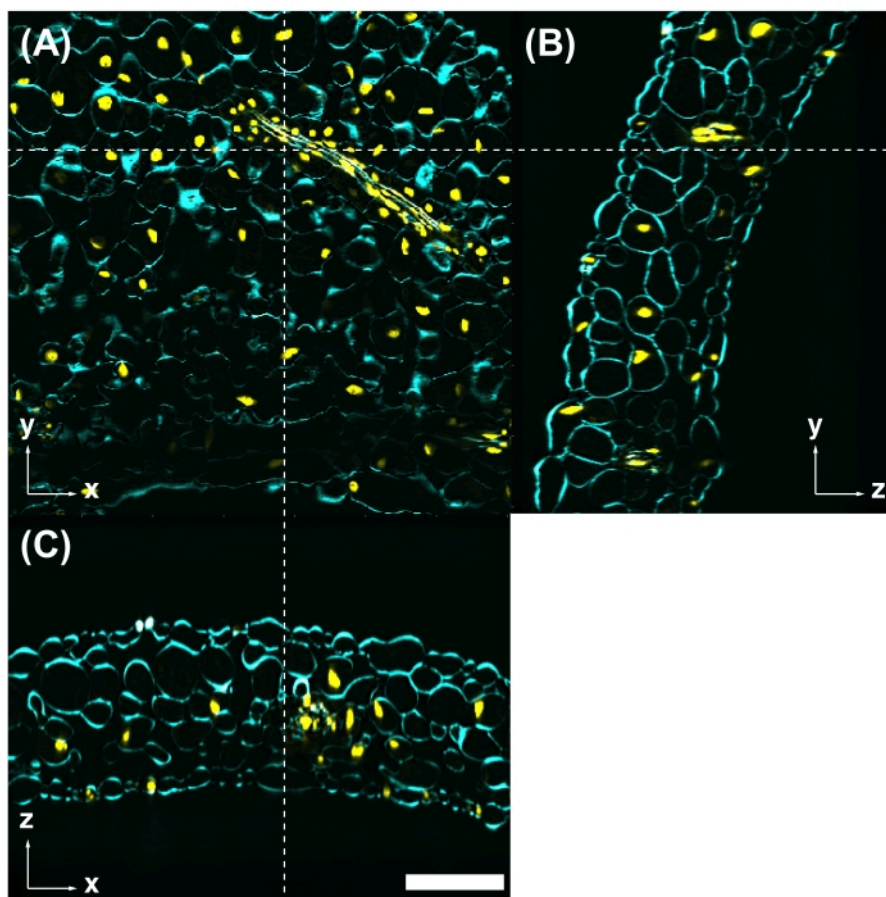


**Figure 5: Fluorescent dye staining is compatible with CS.** (A) CS-treated leaves observed by two-photon excitation microscopy with 950 nm excitation. Cell wall is stained with Calcofluor White (cyan). Nuclei are labeled with UBQ10pro::H2B-mClover (yellow). The yz (B) and xz (C) images are cross-sections at the position indicated by the white dashed lines in (A). Scale bar: 100  $\mu\text{m}$ . [Please click here to view a larger version of this figure.](#)

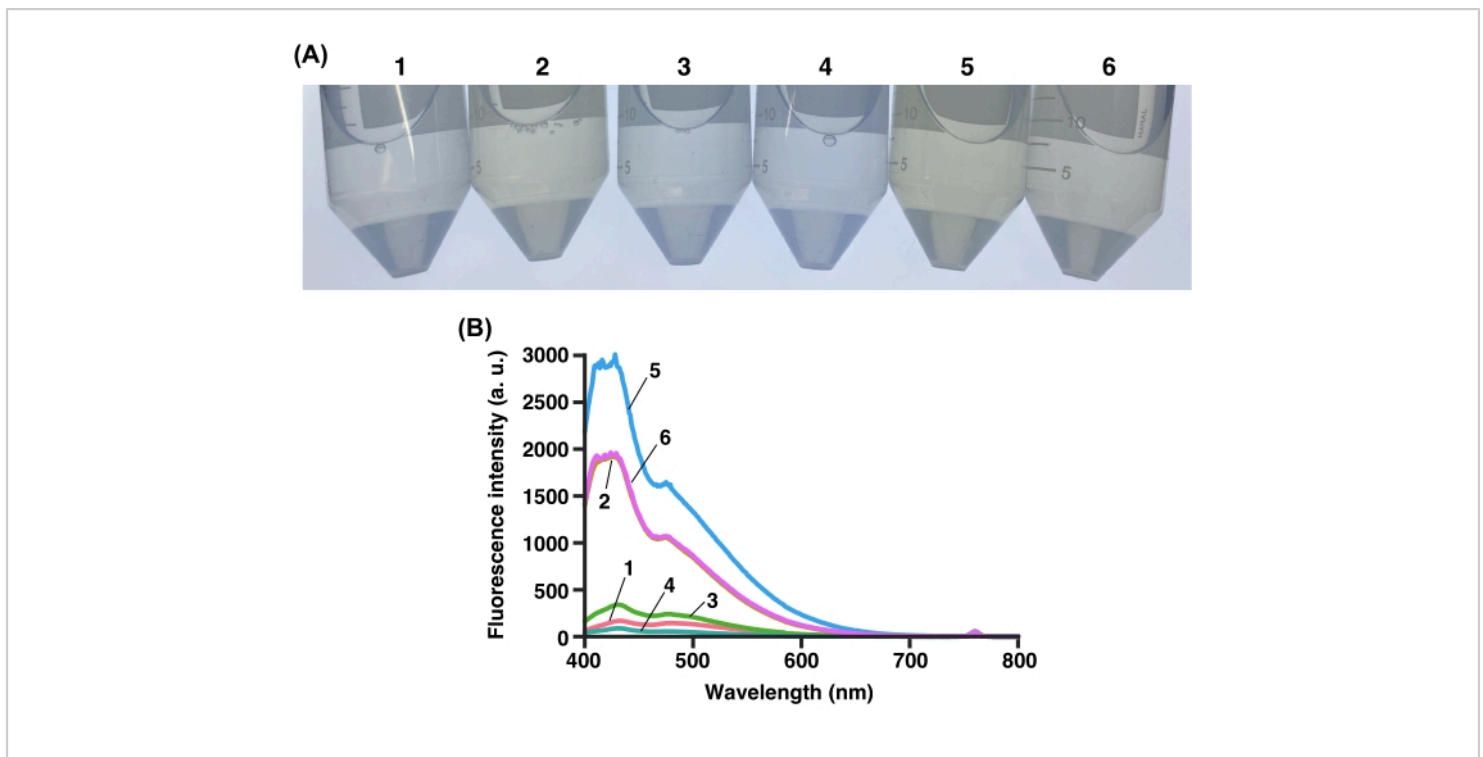


**Figure 6: Transparency of sodium deoxycholate.** (A) Colors of various 15% sodium deoxycholates (listed in **Table of Materials**). (B) Fluorescence spectrum of each 15% sodium deoxycholate with 380 nm excitation. [Please click here to view a larger version of this figure.](#)

## Discussion

This method consists of fixation, washing, and cleaning. Fixation is a critical step in this protocol. If the fluorescent protein is not observed after PFA fixation, it will not be observed after treatment with clearing solution. The penetration of PFA solution into tissues is critical, but high vacuum treatment is not recommended because it can destroy the cell structure. Vacuum conditions and fixation periods should be optimized for each type of tissue and species. It is recommended to check fluorescent proteins even after fixation. Although samples were usually fixed for 30-60 min at room temperature, they can be fixed at 4 °C for a longer time (overnight or more).

As shown in **Figure 6A**, some sodium deoxycholates had a pale-yellow color when dissolved. Such sodium deoxycholate solutions showed strong autofluorescence in the 400-600 nm region after excitation at 380 nm (**Figure 6B**). This autofluorescence prevents optical clearing and fluorescence imaging. Users should check the color of sodium deoxycholate solution as the quality of the reagent might differ owing to purity, lot-to-lot variation, or other reasons.

The clearing solutions used here have high concentrations of sodium deoxycholate, which could destroy the membrane structure. The plasma membrane marker (RPS5Apro::tdTomato-LTI6b) was observed even after CS treatment<sup>7</sup>. However, it might be better to reduce the concentration of sodium deoxycholate, depending on the

structure and tissue of interest. Indeed, images with improved clarity were obtained for *Arabidopsis* pistils with modified CS, in which the concentration of sodium deoxycholate is reduced by half; however, reduced concentrations of sodium deoxycholate required prolonged treatment times (e.g., 1 month for *Arabidopsis* pistils).

CS can reduce red autofluorescence (>610 nm) to remove chlorophyll in treated samples. However, 500-600 nm range autofluorescence (yellow to orange) remained even in CS-treated samples<sup>7</sup>. This autofluorescence is thought to be derived from the cell wall and other cellular components, such as lignin<sup>12,13</sup>. Therefore, it is difficult to make tissues, such as stems with developed secondary walls, completely transparent by CS treatment.

Several clearing reagents besides the ones used here have been developed to observe fluorescent proteins in plants using fluorescent microscopy<sup>14,15,16,17</sup>. Compared with these methods, CS and CSA remove chlorophyll and reduce autofluorescence, making the plant tissues more transparent. Recently, Sakamoto et al. developed an improved method, iTOMEI, for fixation, detergent clearing, and mounting to adjust the refractive index mismatch<sup>18</sup>. In *Arabidopsis* seedlings, iTOMEI cleared the tissue within 26 h.

CS is applicable to a wide range of plant species, such as *Arabidopsis thaliana*, *Physcomitrium patens*<sup>7</sup>, *Chrysanthemum morifolium*, *Cucumis sativus*, *Nicotiana benthamiana*, *Nicotiana tabacum*, *Torenia fournieri*<sup>8</sup>, *Allium ochotense*<sup>19</sup>, *Astragalus sinicus*<sup>20</sup>, avocado<sup>21</sup>, barley<sup>22</sup>, *Brassica rapa*<sup>23</sup>, *Callitriche*<sup>24</sup>, *Eucalyptus*<sup>25</sup>, maize<sup>26</sup>, *Marchantia polymorpha*<sup>27</sup>, *Monophyllaea glabra*<sup>28</sup>, *Orobancha minor*<sup>29</sup>, petunia<sup>30</sup>, rice<sup>31</sup>, *Solanum lycopersicum*<sup>32</sup>, soybean<sup>33</sup>, strawberry<sup>34</sup>, wheat<sup>35</sup>, and *Wolffiella hyalina*<sup>36</sup>. For thicker tissues, CS can also make the

vibratome sections transparent<sup>37,38</sup>. This method allowed studies of the cellular structure and gene expression patterns in plants<sup>37,38</sup>. Moreover, nematode infections<sup>20,39</sup>, fungal infections, and symbiosis<sup>19,40,41</sup> were also observed deep inside the CS-treated tissues. Thus, this method is useful for whole tissue imaging from micro- to macro-scales and could help to discover novel interactions among various cells, tissues, organs, and organisms.

## Disclosures

ClearSee is commercialized (Fujifilm Wako Pure Chemical Corporation, Japan). Nagoya University holds a patent (JP6601842) on the clearing reagent ClearSee. D. Kurihara is the patent inventor. The authors declare no competing financial interests.

## Acknowledgments

This work was supported by the Japan Society for the Promotion of Science (Grant-in-Aid for Scientific Research on Innovative Areas (JP16H06464, JP16H06280 to T.H.), Grant-in-Aid for Scientific Research (B, JP17H03697 to D.K.), Grant-in-Aid for Challenging Exploratory Research (JP18K19331 to D.K.), Grant-in-Aid for Scientific Research on Innovative Areas (JP20H05358 for D.K.)) and the Japan Science and Technology Agency (PRESTO program (JPMJPR15QC to Y.M., JPMJPR18K4 to D.K.)). The authors are thankful to the Live Imaging Center at the Institute of Transformative Bio-Molecules (WPI-ITbM) of Nagoya University for supporting the microscopic studies and Editage (www.editage.com) for English language editing.

## References

1. Vogelmann, T. C. Light within the plant. *Photomorphogenesis in Plants*. 491-535 (1994).

2. Krause, G. H., Weis, E. Chlorophyll fluorescence and photosynthesis: The basics. *Annual Review of Plant Physiology and Plant Molecular Biology*. **42** (1), 313-349 (1991).
3. Pourcel, L., Routaboul, J., Cheynier, V., Lepiniec, L., Debeaujon, I. Flavonoid oxidation in plants: from biochemical properties to physiological functions. *Trends in Plant Science*. **12** (1), 29-36 (2007).
4. Lersten, N. R. An annotated bibliography of botanical clearing methods. *Iowa State Journal of Science*. **41** (4), 481-486 (1967).
5. Villani, T. S., Koroch, A. R., Simon, J. E. An improved clearing and mounting solution to replace chloral hydrate in microscopic applications. *Applications in Plant Sciences*. **1** (5), 1300016 (2013).
6. Becker, K., Jährling, N., Saghafi, S., Weiler, R., Dodt, H.-U. Chemical clearing and dehydration of GFP expressing mouse brains. *PLoS ONE*. **7** (3), e33916 (2012).
7. Kurihara, D., Mizuta, Y., Sato, Y., Higashiyama, T. ClearSee: a rapid optical clearing reagent for whole-plant fluorescence imaging. *Development*. **142** (23), 4168-4179 (2015).
8. Kurihara, D., Mizuta, Y., Nagahara, S., Higashiyama, T. ClearSeeAlpha: advanced optical clearing for whole-plant imaging. *Plant and Cell Physiology*. **62** (8), 1302-1310 (2021).
9. Ursache, R., Andersen, T. G., Marhavý, P., Geldner, N. A protocol for combining fluorescent proteins with histological stains for diverse cell wall components. *The Plant Journal*. **93** (2), 399-412 (2018).
10. Tofanelli, R., Vijayan, A., Scholz, S., Schneitz, K. Protocol for rapid clearing and staining of fixed *Arabidopsis* ovules for improved imaging by confocal laser scanning microscopy. *Plant Methods*. **15** (1), 120 (2019).
11. Vijayan, A. et al. A digital 3D reference atlas reveals cellular growth patterns shaping the *Arabidopsis* ovule. *eLife*. **10**, 1-38 (2021).
12. Müller, S. M., Galliardt, H., Schneider, J., George Barisas, B., Seidel, T. Quantification of Förster resonance energy transfer by monitoring sensitized emission in living plant cells. *Frontiers in Plant Science*. **4**, 1-20 (2013).
13. Mizuta, Y., Kurihara, D., Higashiyama, T. Two-photon imaging with longer wavelength excitation in intact *Arabidopsis* tissues. *Protoplasma*. **252**, 1231-1240 (2015).
14. Littlejohn, G. R., Gouveia, J. D., Edner, C., Smirnoff, N., Love, J. Perfluorodecalin enhances in vivo confocal microscopy resolution of *Arabidopsis thaliana* mesophyll. *New Phytologist*. **186** (4), 1018-1025 (2010).
15. Warner, C. A. et al. An optical clearing technique for plant tissues allowing deep imaging and compatible with fluorescence microscopy. *Plant Physiology*. **166** (4), 1684-1687 (2014).
16. Hasegawa, J. et al. Three-dimensional imaging of plant organs using a simple and rapid transparency technique. *Plant and Cell Physiology*. **57** (3), 462-472 (2016).
17. Musielak, T. J., Slane, D., Liebig, C., Bayer, M. A versatile optical clearing protocol for deep tissue imaging of fluorescent proteins in *Arabidopsis thaliana*. *PLoS ONE*. **11** (8), e0161107 (2016).

18. Sakamoto, Y. et al. Improved clearing method contributes to deep imaging of plant organs. *Research Square*. (2021).
19. Tanaka, E., Ono, Y. Whole-leaf fluorescence imaging to visualize in planta fungal structures of Victory onion leaf rust fungus, *Uromyces japonicus*, and its taxonomic evaluation. *Mycoscience*. **59** (2), 137-146 (2018).
20. Ohtsu, M. et al. Spatiotemporal deep imaging of syncytium induced by the soybean cyst nematode *Heterodera glycines*. *Protoplasma*. **254**, 2107-2115 (2017).
21. Duman, Z. et al. Short de-etiolation increases the rooting of VC801 Avocado rootstock. *Plants*. **9** (11), 1481 (2020).
22. Ho, W. W. H. et al. Integrative multi-omics analyses of barley rootzones under salinity stress reveal two distinctive salt tolerance mechanisms. *Plant Communications*. **1** (3), 100031 (2020).
23. Arsovski, A. A. et al. BrphyB is critical for rapid recovery to darkness in mature *Brassica rapa* leaves. *bioRxiv*. 2020.05.22.111245 (2020).
24. Doll, Y., Koga, H., Tsukaya, H. The diversity of stomatal development regulation in *Callitriche* is related to the intrageneric diversity in lifestyles. *Proceedings of the National Academy of Sciences of the United States of America*. **118** (14), e2026351118 (2021).
25. Eliyahu, A. et al. Vegetative propagation of elite Eucalyptus clones as food source for honeybees (*Apis mellifera*); adventitious roots versus callus formation. *Israel Journal of Plant Sciences*. **67** (1-2), 83-97 (2020).
26. Kelliher, T. et al. MATRILINEAL, a sperm-specific phospholipase, triggers maize haploid induction. *Nature*. **542**, 105-109 (2017).
27. Aki, S. S. et al. Cytokinin signaling is essential for organ formation in *Marchantia polymorpha*. *Plant and Cell Physiology*. **60** (8), 1842-1854 (2019).
28. Kinoshita, A., Koga, H., Tsukaya, H. Expression profiles of *ANGUSTIFOLIA3* and *SHOOT MERISTEMLESS*, key genes for meristematic activity in a one-leaf plant *Monophyllaea glabra*, revealed by whole-mount in situ hybridization. *Frontiers in Plant Science*. **11**, 1-11 (2020).
29. Okazawa, A. et al. Localization of planteose hydrolysis during seed germination of *Orobancha minor*. *bioRxiv*. 2021.06.16.448768 (2021).
30. Chen, M. et al. VAPYRIN attenuates defence by repressing PR gene induction and localized lignin accumulation during arbuscular mycorrhizal symbiosis of *Petunia hybrida*. *New Phytologist*. **229** (6), 3481-3496 (2021).
31. Chu, T. T. H. et al. Sub-cellular markers highlight intracellular dynamics of membrane proteins in response to abiotic treatments in rice. *Rice*. **11**, 23 (2018).
32. Alaguero-Cordovilla, A. et al. An auxin-mediated regulatory framework for wound-induced adventitious root formation in tomato shoot explants. *Plant, Cell & Environment*. **44** (5), 1642-1662 (2021).
33. Okuda, A., Matsusaki, M., Masuda, T., Urade, R. Identification and characterization of GmPDIL7, a soybean ER membrane-bound protein disulfide isomerase family protein. *The FEBS Journal*. **284** (3), 414-428 (2017).
34. Kim, D.-R. et al. A mutualistic interaction between *Streptomyces* bacteria, strawberry plants and pollinating bees. *Nature Communications*. **10** (1), 4802 (2019).

35. Wu, J., Mock, H.-P., Giehl, R. F. H., Pitann, B., Mühling, K. H. Silicon decreases cadmium concentrations by modulating root endodermal suberin development in wheat plants. *Journal of Hazardous Materials*. **364**, 581-590 (2019).
36. Isoda, M., Oyama, T. Use of a duckweed species, *Wolffiella hyalina*, for whole-plant observation of physiological behavior at the single-cell level. *Plant Biotechnology*. **35** (4), 387-391 (2018).
37. Ben-Targem, M., Ripper, D., Bayer, M., Ragni, L. Auxin and gibberellin signaling cross-talk promotes hypocotyl xylem expansion and cambium homeostasis. *Journal of Experimental Botany*. **72** (10), 3647-3660 (2021).
38. Shwartz, I. et al. The VIL gene CRAWLING ELEPHANT controls maturation and differentiation in tomato via polycomb silencing. *bioRxiv*. 2021.06.02.446760 (2021).
39. Levin, K. A., Tucker, M. R., Strock, C. F., Lynch, J. P., Mather, D. E. Three-dimensional imaging reveals that positions of cyst nematode feeding sites relative to xylem vessels differ between susceptible and resistant wheat. *Plant Cell Reports*. **40** (2), 393-403 (2021).
40. Nouri, E. et al. Phosphate suppression of arbuscular mycorrhizal symbiosis involves gibberellic acid signaling. *Plant and Cell Physiology*. **62** (6), 959-970 (2021).
41. Evangelisti, E. et al. Artificial intelligence enables the identification and quantification of arbuscular mycorrhizal fungi in plant roots. *bioRxiv*. 2021.03.05.434067 (2021).